Systematic *ab initio* study of curvature effects in carbon nanotubes

O. Gülseren,[1,2] T. Yildirim,[1] and S. Ciraci[3]

[1] *NIST Center for Neutron Research, National Institute of Standards and Technology, Gaithersburg, Maryland 20899*
[2] *Department of Materials Science and Engineering, University of Pennsylvania, Philadelphia, Pennsylvania 19104*
[3]*Department of Physics, Bilkent University, Ankara 06533, Turkey*
(Received 11 December 2001; published 28 March 2002)

We investigate curvature effects on geometric parameters, energetics, and electronic structure of zigzag nanotubes with fully optimized geometries from first-principle calculations. The calculated curvature energies, which are inversely proportional to the square of radius, are in good agreement with the classical elasticity theory. The variation of the band gap with radius is found to differ from simple rules based on the zone folded graphene bands. Large discrepancies between tight binding and first-principles calculations of the band gap values of small nanotubes are discussed in detail.

I. INTRODUCTION

Single wall carbon nanotubes (SWNT's) are basically rolled graphite sheets, which are characterized by two integers (n,m) defining the rolling vector of graphite.[1] Therefore, electronic properties of SWNT's, at first order, can be deduced from that of graphene by mapping the band structure of two dimensional (2D) hexagonal lattice on a cylinder.[1–5] Such analysis indicates that the (n,n) armchair nanotubes are always metal and exhibit one dimensional quantum conduction.[6] The $(n,0)$ zigzag nanotubes are generally semiconductor and only are metal if n is an integer multiple of three. However, recent experiments[7] indicate much more complicated structural dependence of the band gap and electronic properties of SWNT's. The semiconducting behavior of SWNT's has been of particular interest, since the electronic properties can be controlled by doping or implementing defects in a nanotube-based optoelectronic devices.[8–14] It is therefore desirable to have a good understanding of electronic and structural properties of SWNT's and the interrelations between them.

Band calculations of SWNT's were initially performed by using a one-band π-orbital tight binding model.[2] Subsequently, experimental data[15–18] on the band gaps were extrapolated to confirm the inverse proportionality with the radius of the nanotube.[5] Later, first-principles calculation[19] within local density approximation (LDA) showed that the σ^*-π^* hybridization becomes significant at small R (or at high curvature). Such an effect were not revealed by the π-orbital tight-binding bands. Recent analytical studies[20–22] showed the importance of curvature effects in carbon nanotubes. Nonetheless, band calculations performed by using different methods have been at variance on the values of the band gap. While recent studies predict interesting effects, such as strongly local curvature dependent chemical reactivity,[14] an extensive theoretical analysis of the curvature effects on geometric and electronic structure has not been carried out so far.

In this paper, we present a systematic *ab initio* analysis of the band structure of zigzag SWNT's showing interesting curvature effects. Our analysis includes a large number of zigzag SWNT's with n ranging from 4 to 15. The fully op-

timized structural and electronic properties of SWNT's are obtained from extensive first-principle calculations within the generalized gradient approximation[23] (GGA) by using pseudopotential planewave method.[24] We used plane waves up to an energy of 500 eV and ultrasoft pseudopotentials.[25] The calculated total energies converged within 0.5 meV/ atom. More details about the calculations can be found in Refs. 26,27.

II. GEOMETRIC STRUCTURE

First, we discuss effects of curvature on structural parameters such as bond lengths and angles. Figure 1 shows a schematic side view of a zigzag SWNT which indicates two types of C-C bonds and C-C-C bond angles, respectively. The curvature dependence of the fully optimized structural parameters of zigzag SWNT's are summarized in Fig. 2. The variation of the normalized bond lengths (i.e., $d_{\text{C-C}}/d_0$ where d_0 is the optimized C-C bond length in graphene) and the bond angles with tube radius R (or n) are shown in Figs. 2(a)
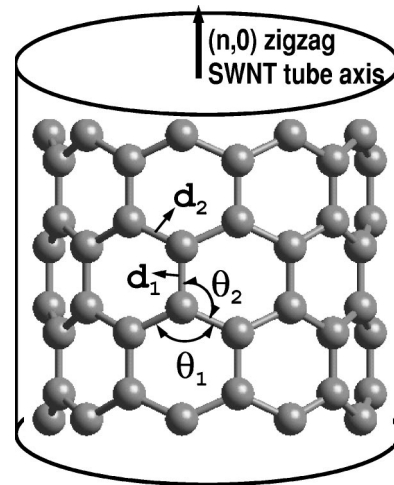

FIG. 1. A schematic side view of a zigzag SWNT, indicating two types of C-C bonds and C-C-C bond angles. These are labeled as d_1, d_2, θ_1, and θ_2. Radius dependence of these variables are important in tight-binding description of SWNT's as discussed in the text.
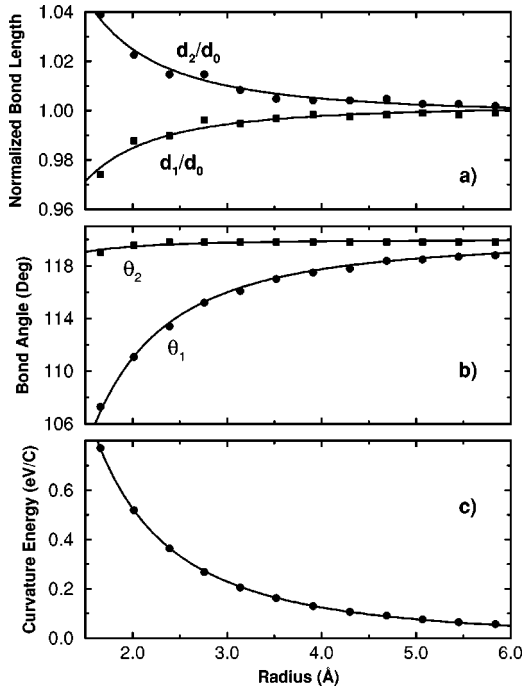
FIG. 2. (a) Normalized bond lengths (d_1/d_0 and d_2/d_0) versus the tube radius R ($d_0 = 1.41$ Å). (b) The bond angles (θ_1 and θ_2) versus R. (c) The curvature energy, E_c per carbon atom with respect to graphene as a function of tube radius. The solid lines are the fit to the data as $1/R^2$.

and 2(b), respectively. Both the bond lengths and the bond angles display a monotonic variation and approach the graphene values as the radius increases. As pointed out earlier for the armchair SWNT's,[28] the curvature effects, however, become significant at small radii. The zigzag bond angle (θ_1) decreases with decreasing radius. It is about 12° less than 120°, namely, the bond angle between sp^2 bonds of the graphene, for the (4,0) SWNT, the smallest tube we studied. The length of the corresponding zigzag bonds (d_2), on the other hand, increases with decreasing R. On the other hand, the length of the parallel bond (d_1) decreases to a lesser extent with decreasing R, and the angle involving this bond (θ_2) is almost constant.

An internal strain is implemented upon the formation of tubular structure from the graphene sheet. The associated strain energy, which is specified as the curvature energy E_c is calculated as the difference of total energy per carbon atom between the bare SWNT and the graphene (i.e., $E_c = E_{T,\text{SWNT}} - E_{T,\text{graphene}}$) for $4 \leq n \leq 15$. The calculated curvature energies are shown in Fig. 2(c). As expected E_c is positive and increases with increasing curvature. Consequently, the binding (or cohesive) energy of carbon atom in a SWNT decrease with increasing curvature. We note that in the classical theory of elasticity the curvature energy is given by the following expression:[29–31]

$$E_c = \frac{Yh^3}{24} \frac{\Omega}{R^2} = \frac{\alpha}{R^2}.$$ (1)

Here Y is the Young's modulus, h is the thickness of the tube, and Ω is the atomic volume. Interestingly, the *ab initio* curvature energies yield a perfect fit to the relation α/R^2 as seen in Fig. 2(c). This situation suggests that the classical theory of elasticity can be used to deduce the elastic properties of SWNT's. In this fit α is found to be 2.14 eV Å^2/atom, wherefrom Y can be calculated with an appropriate choice of h.

III. ELECTRONIC STRUCTURE

An overall behavior of the electronic band structures of SWNT's has been revealed from zone folding of the graphene bands.[2–4] Accordingly, all $(n,0)$ zigzag SWNT were predicted to be metallic when n is multiple of 3, since the double degenerate π and π^* states, which overlap at the K point of the hexagonal Brillouin zone (BZ) of graphene folds to the Γ point of the tube.[2,4] This simple picture provides a qualitative understanding, but fails to describe some important features, in particular for small radius or *metallic* nanotubes. This is clearly shown in Table I, where the band gaps calculated in the present study are summarized and compared with results obtained from other methods in the literature. For example, our calculations result in small but non-zero energy band gaps of 93, 78, and 28 meV for (9,0), (12,0), and (15,0) SWNT's, respectively (see Table I). Recently, these gaps were measured by scanning tunneling spectroscopy (STS) experiments[7] as 80, 42, and 29 meV, in the same order. The biggest discrepancy noted in Table I is between the tight-binding and the first-principles values of

TABLE I. Band gap E_g as a function of radius R of $(n,0)$ zigzag nanotubes. M denotes the metallic state. Present results for E_g were obtained within GGA. First row of Ref. 19 is LDA results while all the rest are tight-binding (TB) results. Two rows of Ref. 33 are for two different TB parametrization.

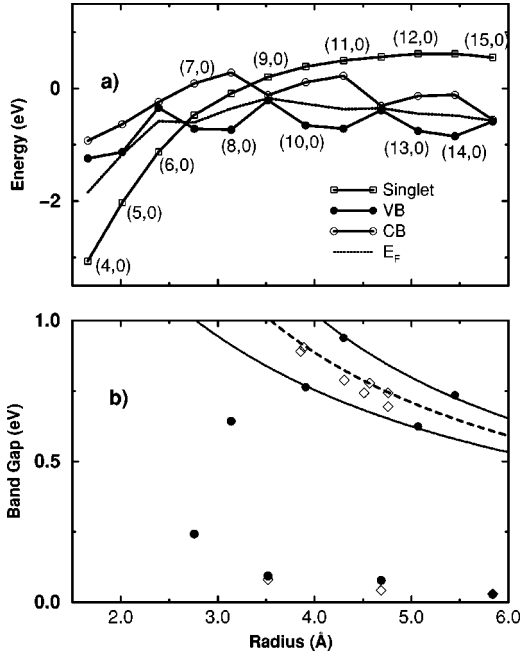| n	4	5	6	7	8	9	10	11	12	13	14	15
R (Å)	1.66	2.02	2.39	2.76	3.14	3.52	3.91	4.30	4.69	5.07	5.45	5.84
E_g (eV)	M	M	M	0.243	0.643	0.093	0.764	0.939	0.078	0.625	0.736	0.028
Ref. 19			M	0.09	0.62	0.17						
Ref. 19			0.05	1.04	1.19	0.07						
Ref. 2			0.21	1.0	1.22	0.045	0.86	0.89	0.008	0.697	0.7	0.0
Ref. 33				0.79	1.12		0.65	0.80				
Ref. 33				1.11	1.33		0.87	0.96				

FIG. 3. (a) Energies of the double degenerate π states (VB), the double degenerate π^* states (CB), and the singlet π^* state as a function of nanotube radius. Each data point corresponds to n ranging from 4 to 15 consecutively. (b) The calculated band gaps as a function of the tube radius shown by filled symbols. Solid (dashed) lines are the plots of Eq. (3) [Eq. (2)]. The experimental data are shown by open diamonds (Refs. 7, 17,18).

the gaps for small radius tubes such as (7,0). These results indicate that curvature effects are important and the simple zone folding picture has to be improved. Moreover, the analysis of the LDA bands of the (6,0) SWNT calculated by Blase *et al.*[19] brought another important effect of the curvature. The antibonding singlet π^* and σ^* states mix and repel each other in curved graphene. As a result, the purely π^* state of planar graphene is lowered with increasing curvature. For zigzag SWNT's, the energy of this singlet π^* state is shifted downwards with decreasing R (or increasing curvature). Here, we extended the analysis of Blase *et al.*[19] to the $(n,0)$ SWNT's with $4 \leq n \leq 15$ by performing GGA calculations.

In Fig. 3(a), we show the double degenerate π states (which are the valence band edge at the Γ point), the double degenerate π^* states (which become the conduction band edge at Γ for large R), and the singlet π^* state (which is in the conduction band for large R). As seen, the shift of the singlet π^* state is curvature dependent, and below a certain radius determines the band gap. For tubes with radius greater than 3.3 Å (i.e., $n > 8$), the energy of the singlet π^* state at the Γ point of the BZ is above the doubly degenerate π^* states (i.e., bottom of the conduction band), while it falls between the valence and conduction band edges for $n = 7,8$, and eventually dips even below the double degenerate valence band π states for the zigzag SWNT with radius less than 2.7 Å (i.e., $n < 7$). Therefore, all the zigzag tubes with radius less than 2.7 Å are metallic. For $n = 7,8$, the edge of the conduction band is made by the singlet π^* state, but not

by the double degenerate π^* state. The band gap derived from the zone folding scheme is reduced by the shift of this singlet π^* state as a result of curvature induced σ^*-π^* mixing. This explains why the tight binding calculations predict band gaps around 1 eV for $n = 7,8$ tubes while the self-consistent calculations predict much smaller value.

Another issue we next address is the variation of the band gap E_g as a function of tube radius. Based on the π-orbital tight binding model, it was proposed[5] that E_g behaves as

$$E_g = \gamma_0 \frac{d_0}{R}, \qquad (2)$$

which is independent from helicity. Within the simple π-orbital tight binding model, γ_0 is taken to be equal to the hopping matrix element $V_{pp\pi}$. (d_0 is the bond length in graphene.) However, as seen in Fig. 3(b), the band gap displays a rather oscillatory behavior up to radius 6.0 Å. The relation given in Eq. (2) was obtained by a second order Taylor expansion of one-electron eigenvalues of the π-orbital tight binding model[5] around the K point of the BZ, and hence it fails to represent the effect of the helicity. By extending the Taylor expansion to the next higher order, Yorikawa and Muramatsu[32,33] included another term in the empirical expression of the band gap variation

$$E_g = V_{pp\pi} \frac{d_0}{R} \left[1 + (-1)^p \gamma \cos(3\theta) \frac{d_0}{R} \right], \qquad (3)$$

which depends on the chiral angle θ as well as an index p. Here γ is a constant and the index p is defined as the integer from $k = n - 2m = 3q + p$. The factor $(-1)^p$ comes from the fact that the allowed $\mathbf{k}$ is nearest to either the K or K' point of the hexagonal Brillouin zone. For zigzag nanotubes studied here, the chiral angle is zero, so the second term just gives R^{-2} dependence as $\pm \gamma V_{pp\pi}(d_0/R)^2$. Hence, the solid lines in Fig. 3(b) are fits to the empirical expression $E_g = V_{pp\pi}d_0/R \pm V_{pp\pi}\gamma d_0^2/R^2$, obtained from Eq. (3) for $\theta = 0$ by using the parameters $V_{pp\pi} = 2.53$ eV and $\gamma = 0.43$. The experimental data obtained by STS (Refs. 17,18) are shown by open diamonds in the same figure. The agreement between our calculations and the experimental data is very good considering the fact that there might be some uncertainties in identifying the nanotube [i.e., assignment of (n,m) indices] in the experiment. The fit of this data to the empirical expression given by Eq. (2) are also presented by a dashed line for comparison.

The situation displayed in Fig. 3 indicates that the variation of the band gap with the radius is not simply $1/R$, but additional terms incorporating the chirality dependence are required. Most importantly, the mixing of the singlet π^* state with the the singlet σ^* state due to the curvature, and its shift towards the valence band with increasing curvature is not included in neither the π orbital tight binding model, nor the empirical relations expressed by Eqs. (2) and (3). This behavior of the singlet π^* states is of particular importance for the applied radial deformation that modifies the curvature and in turn induces metallization.[12,27,34]

In conclusion, we investigated structural and electronic properties that result from the tubular nature of the SWNT's. The first-principles total energy calculations indicated that significant amount of strain energy is implemented in a SWNT when the radius is small. However, the elastic properties can be still described by the classical theory of elasticity. We showed how the singlet π^* state in the conduction band of a zigzag tube moves and eventually enters in the band gap between the doubly degenerate π^*-conduction and π-valence bands. As a result, the energy band structure and the variation of the gap with radius (or n) differs from what one derived from the zone folded band structure of graphene based on the simple tight binding calculations.

[1] M.S. Dresselhaus, G. Dresselhaus, and P.C. Eklund, *Science of Fullerenes and Carbon Nanotubes* (Academic Press, San Diego, 1996); R. Saito, G. Dresselhaus, and M.S. Dresselhaus, *Physical Properties of Carbon Nanotubes* (Imperial College Press, London, 1998).

[2] N. Hamada, S. Sawada, and A. Oshiyama, Phys. Rev. Lett. **68**, 1579 (1992).

[3] M.S. Dresselhaus, G. Dresselhaus, and R. Saito, Phys. Rev. B **45**, 6234 (1992).

[4] J.W. Mintmire, B.I. Dunlap, and C.T. White, Phys. Rev. Lett. **68**, 631 (1992).

[5] C.T. White, D.H. Robertson, and J.W. Mintmire, Phys. Rev. B **47**, 5485 (1993).

[6] S. Frank, P. Poncharal, Z.L. Wang, and W.A. Heer, Science **280**, 1744 (1998); for a recent review, S. Ciraci, A. Buldum, and I. Batra, J. Phys.: Condens. Matter **13**, 537 (2001).

[7] M. Ouyang, J. Huang, C.L. Cheung, and C.M. Lieber, Science **292**, 702 (2001).

[8] L. Chico, M.P. Lopez Sancho, and M.C. Munoz, Phys. Rev. Lett. **81**, 1278 (1998).

[9] P.G. Collins, A. Zettl, H. Bando, A. Thess, and R.E. Smalley, Science **278**, 100 (1997).

[10] M. Bockrath, D.H. Cobden, P.L. McEuen, N.G. Chopra, A. Zettl, A. Thess, and R.E. Smalley, Science **275**, 1922 (1997).

[11] A. Bezryadin, A.R.M. Verschueren, S.J. Tans, and C. Dekker, Phys. Rev. Lett. **80**, 4036 (1998).

[12] Ç. Kılıç, S. Ciraci, O. Gülseren, and T. Yildirim, Phys. Rev. B **62**, 16 345 (2000).

[13] H.S. Sim, C.J. Park, and K.J. Chang, Phys. Rev. B **63**, 073402 (2001).

[14] O. Gülseren, T. Yildirim, and S. Ciraci, Phys. Rev. Lett. **87**, 116802 (2001).

[15] J.W.G. Wildöer, L.C. Venema, A.G. Rinzler, R.E. Smalley, and C. Dekker, Nature (London) **391**, 59 (1998).

[16] L.C. Venema, J.W. Janssen, M.R. Buitelaar, J.W.G. Wildöer, S.G. Lemay, L.P. Kouwenhoven, and C. Dekker, Phys. Rev. B **62**, 5238 (2000).

[17] T.W. Odom, J. Huang, P. Kim, and C.M. Lieber, Nature (London) **391**, 62 (1998).

[18] T.W. Odom, J. Huang, P. Kim, and C.M. Lieber, J. Phys. Chem. B **104**, 2794 (2000).

[19] X. Blase, L.X. Benedict, E.L. Shirley, and S.G. Louie, Phys. Rev. Lett. **72**, 1878 (1994).

[20] C.L. Kane and E.J. Mele, Phys. Rev. Lett. **78**, 1932 (1997).

[21] A. Kleiner and S. Eggert, Phys. Rev. B **63**, 073408 (2001).

[22] A. Kleiner and S. Eggert, Phys. Rev. B **64**, 113402 (2001).

[23] J.P. Perdew and Y. Wang, Phys. Rev. B **46**, 6671 (1992).

[24] M.C. Payne, M.P. Teter, D.C. Allen, T.A. Arias, and J.D. Joannopoulos, Rev. Mod. Phys. **64**, 1045 (1992).

[25] D. Vanderbilt, Phys. Rev. B **41**, 7892 (1990).

[26] T. Yildirim, O. Gülseren, Ç. Kılıç, and S. Ciraci, Phys. Rev. B **62**, 12648 (2000); T. Yildirim, O. Gülseren, and S. Ciraci, *ibid.* **64**, 075404 (2001).

[27] O. Gülseren, T. Yildirim, S. Ciraci, and Ç. Kılıç, Phys. Rev. B **65**, 155410 (2002).

[28] D. Sanchez-Portal, E. Artacho, J.M. Soler, A. Rubio, and P. Ordejon, Phys. Rev. B **59**, 12 678 (1999).

[29] D.H. Robertson, D.W. Brenner, and J.W. Mintmire, Phys. Rev. B **45**, 12 592 (1992).

[30] G.G. Tibbets, J. Cryst. Growth **66**, 632 (1984).

[31] K.N. Kudin, G.E. Scuseria, and B.I. Yakobson, Phys. Rev. B **64**, 235406 (2001).

[32] H. Yorikawa and S. Muramatsu, Solid State Commun. **94**, 435 (1995).

[33] H. Yorikawa and S. Muramatsu, Phys. Rev. B **52**, 2723 (1995).

[34] C.J. Park, Y.H. Kim, and K.J. Chang, Phys. Rev. B **60**, 10 656 (1999).